REPORT DOCUMENTATION PAGE

Form Approved
OMB No. 0704-0188

1. REPORT DATE *(MM/DD/YYYY)*	**2. REPORT TYPE**	**3. DATES COVERED** *(From - To)*
	Technical Paper	

4. TITLE AND SUBTITLE
Detonation Wave Driven by Aerosolized Liquid RP-2 Spray

5a. CONTRACT NUMBER

5b. GRANT NUMBER

5c. PROGRAM ELEMENT NUMBER

6. AUTHOR(S)
Vidhan Malik, Sheikh Salauddin, Rachel Hytovick, Kareem Ahmed, Ral Bielawski, Venkat Raman, John Bennewitz, Jason Burr, Eric Paulson, and William Hargus

5d. PROJECT NUMBER

5e. TASK NUMBER

5f. WORK UNIT NUMBER
Q1UQ

7. PERFORMING ORGANIZATION NAME(S) AND ADDRESS(ES) AND ADDRESS(ES)
University of Central Florida
University of Toronto
University of Michigan
Air Force Research Laboratory, Edwards AFB

8. PERFORMING ORGANIZATION REPORT NO.

9. SPONSORING / MONITORING AGENCY NAME(S) AND ADDRESS(ES)
Air Force Research Laboratory
Rocket Propulsion Division
5 Pollux Drive
Edwards AFB, CA 93524

10. SPONSOR/MONITOR'S ACRONYM(S)
RQRC

11. SPONSOR/MONITOR'S REPORT NUMBER(S)
AFRL-RQ-ED-TP-2021-314

12. DISTRIBUTION / AVAILABILITY STATEMENT
DISTRIBUTION STATEMENT A. Approved for public release. Distribution is unlimited.

13. SUPPLEMENTARY NOTES
Public Affairs Clearance Number: AFRL-2021-4322; Clearance Date 6 Dec 2021.
Presented at 39th International Symposium on Combustion, Vancouver, Canada, 24-29 July 2022
This material is based on work supported by the Air Force Research Laboratory.

14. ABSTRACT

Detonation-based engines such as Rotating Detonating Engines (RDEs) have been of significant interest for aerospace propulsion. However, most detonation-related studies have focused on gaseous reactants with recent investigations focusing on liquid water interactions with gaseous detonations and shocks. This study explores the dynamics of detonation waves driven by aerosolized liquid fuel sprays. An Unlike-Doublet impinging-jet injector is used to atomize RP-2 and water into aerosolized liquid droplet cloud of measured droplet size distribution where the detonation wave interacts with the cloud mixture. Evidence of RP-2 driving the detonation phenomenon is quantified using dynamic pressure measurements and four simultaneous optical diagnostic measurements: high-speed schlieren, CH* chemiluminescence, formaldehyde planar laser-induced fluorescence (PLIF), and particle Mie scatter. The results show formaldehyde and CH* generation along with a substantial increase in pressure and wave speed when the detonation wave interacts with the RP2 mixture cloud. On the contrary, the detonation pressure and wave speed decrease are observed when the detonation wave interacts with the water droplet cloud. The investigation provides supporting information on liquid fuel droplet burning and heat release driving the detonation wave.

15. SUBJECT TERMS
Pressure Gain Combustion; Liquid Detonations; Liquid Rotating Detonation Rocket Engines; Multiphase Detonations; Optical Diagnostics

16. SECURITY CLASSIFICATION OF:			**17. LIMITATION OF ABSTRACT**	**18. NUMBER OF PAGES**	**19a. NAME OF RESPONSIBLE PERSON**
					John Bennewitz
a. REPORT	**b. ABSTRACT**	**c. THIS PAGE**	SAR	10	**19b. TELEPHONE NO** *(include area code)*
Unclassified	**Unclassified**	**Unclassified**			N/A

Detonation Wave Driven by Aerosolized Liquid RP-2 Spray

Vidhan Malik[a], Sheikh Salauddin[a], Rachel Hytovick[a], Kareem Ahmed[a], Ral Bielawski[b], Venkat Raman[b], John Bennewitz[c], Jason Burr[c], Eric Paulson[c], William Hargus[c]

[a]*University of Central Florida*
[b]*University of Michigan*
[c]*Air Force Research Laboratory*

Abstract

Detonation-based engines such as Rotating Detonating Engines (RDEs) have been of significant interest for aerospace propulsion. However, most detonation-related studies have focused on gaseous reactants with recent investigations focusing on liquid water interactions with gaseous detonations and shocks. This study explores the dynamics of detonation waves driven by aerosolized liquid fuel sprays. An Unlike-Doublet impinging-jet injector is used to atomize RP-2 and water into aerosolized liquid droplet cloud of measured droplet size distribution where the detonation wave interacts with the cloud mixture. Evidence of RP-2 driving the detonation phenomenon is quantified using dynamic pressure measurements and four simultaneous optical diagnostic measurements: high-speed schlieren, CH* chemiluminescence, formaldehyde planar laser-induced fluorescence (PLIF), and particle Mie scatter. The results show formaldehyde and CH* generation along with a substantial increase in pressure and wave speed when the detonation wave interacts with the RP2 mixture cloud. On the contrary, the detonation pressure and wave speed decrease are observed when the detonation wave interacts with the water droplet cloud. The investigation provides supporting information on liquid fuel droplet burning and heat release driving the detonation wave.

Keywords: Pressure Gain Combustion; Liquid Detonations; Liquid Rotating Detonation Rocket Engines; Multiphase Detonations; Optical Diagnostics;

---

*Corresponding author.
Email addresses: vidmalik@Knights.ucf.edu *(V. Malik),* sheikh_salauddin.ucf@knights.ucf.edu *(S. Salauddin),* rhytovick@knights.ucf.edu *(R.Hytovick),* kareem.ahmed@ucf.edu *(K. Ahmed)*

1. Introduction

Recent scientific advances reinvigorated studies of advanced propulsion devices. Detonation-based engines have been shown to theoretically provide a viable solution to reaching high thermodynamic efficiencies. This increase in efficiency is due to detonation systems operating on a pseudo-constant volume cycle instead of the conventional constant pressure Brayton cycle in gas turbines [1, 2]. The larger thermodynamic efficiency results from the detonation reaction mechanism where shock compression significantly increases the pressure and density of the reactants. Exothermic reactions then rapidly expand the gases in a confined volume, resulting in the sustenance for the shock, which supports the pressure gain process. For this reason, detonations are typically classified as a form of pressure gain combustion. Generally, thermodynamic cycles are typically associated with the entire system (i.e., compressor, combustion, and turbine), but for this description, we focus on the detonation wave combustion, not the entire system.

Thus far, detonation research has predominantly been focused on using gaseous reactants due to the complexities of testing and analyzing liquid spray detonations. In particular, liquid spray-assisted detonations pose a unique challenge to quantifying the associated pressure gain because of the complex theoretical modeling needed to understand the underlying intricate flow physics of the spray interaction with the detonation wave structure. Liquid spray interaction was first investigated in the 1960s theoretically by F.A. Williams, then followed experimentally by K. W. Ragland [3, 4]. Since then, there have been various investigations conducted regarding liquid spray detonations. Yao *et al.* studied the impact of hydrocarbon fuel and air mixtures on initiation and detonation cell size and reported a relationship classified following a 'U' behavior relative to equivalence ratio [5]. It was subsequently followed up by Benmahammed *et al.*, who utilized isooctane-air sprays to study the cellular detonation structure experimentally and numerically using 30 μm diameter droplets and documented three detonation regimes as equivalence ratio was increased; spinning, half-cell structure, and multi-headed detonation regime [6]. Recently, Jarsale *et al.* experimentally explored the effects of a mean 10 μm diameter water spray on an ethylene-air detonation wave relative to detonation wave structures and cell sizes and found that cell size increased dramatically while hydrodynamic thickness remained constant [7]. Since then, efforts in large have been focused on numerical simulation of liquid droplet impact on detonation waves, highlighting velocity deficit and enlarged hydrodynamic thicknesses [8]. Due to the growing interest in multiphase detonations, new experimental studies with high-speed and better resolution imaging/diagnostics from the community are needed to comprehend the phenomenon further.

There is significant interest in employing liquid fuels in detonation-based propulsion systems such as rotating detonating engines (RDEs), especially hydrocarbons, due to their higher energy density content. In this study, the dynamics of a detonation wave interacting with aerosolized liquid fuel sprays are explored. An unlike-doublet impinging-jet injector that would be used for a liquid rotating detonation rocket engine is used to atomize RP-2 and water. The droplet size distribution of the aerosolized liquid droplet cloud of the injector is characterized. The effect of the aerosolized liquid droplet cloud on the detonation is characterized using laser and optical diagnostics along with pressure measurements. The results show clear evidence of formaldehyde and CH* generated by the RP-2 burning as the detonation interacts with the aerosolized cloud. Additionally, the wave speed and pressure increases corresponding to the heat release from the RP-2. This is contrary to the water aerosolized cloud which is expected. A theoretical analysis is provided for the burning of the RP-2 droplets within the wavefront.

2. Experiment and diagnostics

2.1 Experimental facility

The 1.5 m long stainless-steel Turbulent Shock Tube (TST), located at the University of Central Florida, as portrayed schematically in Fig. 1, was used to initiate detonations for the current research investigation [9, 10]. The TST is a semi-confined experimental facility that houses a test section to provide 102 mm of optical access through a portion of its 45 mm^2 square cross-section. The test section has full optical access via three fused silica windows, allowing more than a 95% transmission rate for advanced laser diagnostics. The TST also encapsulates a 0.6-meter turbulence generator containing a series of 58% open area perforated plates that induce turbulent flame acceleration and transition the flame from the initial slow deflagration state to the final detonation formation. A spark plug is mounted on the center-axis at the system head end, which initiates the combustion reaction.

Fig. 1: Schematic of experimental facility

2.2 Unlike-Doublet Injector

An Unlike-Doublet impinging rocket injector with liquid RP-2 and gaseous supersonic oxygen jet is used for the investigation. This type of injector is used due to its ability to efficiently generate an aerosolized

droplet cloud and relevance to RDEs. The injector is mounted to the top of the test section positioned between pressure transducers P2 and P3, as shown in

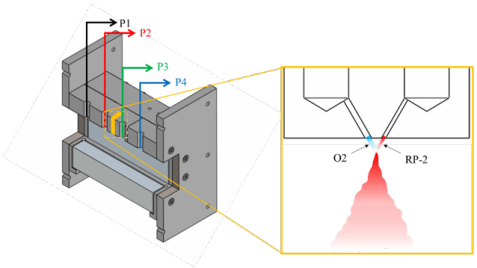

Fig. 2:Unlike-doublet atomizing injector used in this study with a corresponding schematic showing the internal geometry and location of four pressure transducers labeled P1, P2, P3, and P4.

Fig. 2. This injector location provides a resolved pressure trace that captures the before and after interaction of the spray and detonation wave. The impingement angle of the gaseous O_2 and liquid RP-2 is 30 degrees from the vertical normal coordinate axis, which induces a supersonic driven atomization breakup mechanism. The oxidizer and liquid channels have diameters of 0.8 and 0.5 mm, respectively. Both channels were supplied with an upstream pressure of 100 psi, which resulted in a vertical spray. The droplet characteristics of the injector were independently investigated utilizing a Phase Doppler Particle Analyzer (PDPA). As shown in the particle size distribution in Fig. 3, the injector produced an average droplet diameter of 20 μm for both water and RP-2. This measured average droplet diameter falls within an ideal range for aiding a detonation phenomenon, as

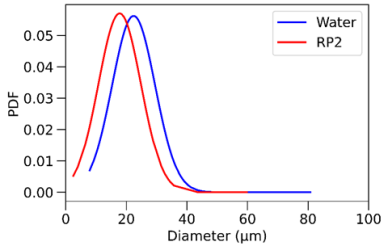

Fig. 3:PDF of Unlike-doublet injector shows a mean droplet diameter of 20 μm for both water and RP-2 for varying mass flow rates.

previously modeled theoretically by Gubin, who shows that diameters below 30 μm can sustain detonations near CJ velocities [11].

2.3 *Flow Control*

A precisely timed flow control system was devised to produce a homogeneous mixture containing hydrogen, oxygen, and air in the experimental facility. The arrangement consisted of rotameters and pressure regulators which metered the reactant flow into the test facility at a nominal mass fraction of 3.1% H_2, 33.5% O_2, and 63.4% N_2. The gases were introduced into the configuration at rates of 3.4 ±0.2, 5 ±0.5, and 25 ±1 SCFH for H_2, O_2, and N_2, respectively, for 30 seconds. The experiment and the mixture composition are designed to isolate the RP-2 hydrocarbon burning using the diagnostics described below. After the entire facility is filled with the fuel-oxidizer mixture, a BNC 575 Pulse/Delay Generator with preset discretized delays is used to send signals to activate the solenoid valves to the injector, spark plug, and cameras to initiate and record the incipient detonation.

2.4 *Experimental Procedures*

The timing of various components and the order in which they are triggered relative to each other are controlled via a BNC 575 Pulse/Delay Generator and LabVIEW. The testing facility is first filled using the aforementioned mixture composition for the 30 s, followed by a 23 ms spark issued in the head end of the facility. Simultaneously, the data is acquired via high-frequency pressure transducers. The spark ignites the mixture and through the turbulence generator, a detonation is formed. An optimized short delay between the spark plug signal and the start of the RP-2 injector spray is issued to minimize the time between the operation of the spray and detonation arrival in the test section. In addition, the delay was configured to ensure the spray had sufficient time to reach a steady-state and mitigate any liquid buildup on the test section walls. Following the delay, schlieren, CH*, Formaldehyde, and Mie Scatter cameras are triggered simultaneously so that the first frame capture the leading shock in the desired location.

2.5 *Diagnostics*

Schlieren imaging was utilized to quantify detonation wave propagation velocity and shock front. The standard Z formation employing two 6-inch diameter parabolic mirrors with a focal length of 60 in. is used to capture the entire test section as shown in Fig. 4. The images were captured and recorded at a rate of 200kHz via a Photron SAZ camera with 16-bit depth and a spatial resolution of 512 X 512 pixels. A Nikon lens with a focal length of 80-200mm F/2.8 was attached to the camera generating an image resolution 217 μm/pix. The uncertainty associated with measuring pixel-based shock velocity was 43 m/s.

CH* Chemiluminescence and Planar Laser-Induced Fluorescence (PLIF) were implemented to investigate regions in the flow field pertaining to hydrocarbon reactions. CH* radical species were captured via a Photron SA-Z camera at a rate of 200kHz with a 24-85mm F/3.5-4.5 Nikon Lens, resulting in an image resolution of 294 μm/pix. A 414 nm bandpass optical filter with a full-width half-

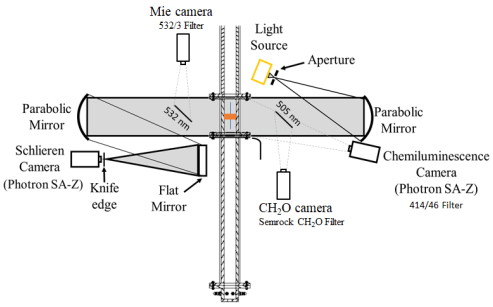

Fig. 4: Schematic of optical setup

maximum of 46 nm and a transmission greater than 98% was mounted to the lens to capture the specific CH* emission wavelength as seen in Fig. 4. For Formaldehyde PLIF, the formaldehyde species within the reaction front were excited using an ND:YAG 355nm, 60 mJ laser. A planar laser sheet intersected the center of the test section and RP-2 spray was created by passing a 355nm laser beam through the center of the test section. The PLIF images were acquired utilizing a CCD camera sensor at a spatial resolution of 20 μm/pix. A 50mm F/1.2 Nikon lens with an attached Semrock 11-band bandpass filter enhanced the peaks of CH_2O emission over the 380 – 480nm wavelength range is used to capture the fluorescence signal. Mounted between the lens and the camera is a LaVision High-Speed IRO-X Intensifier operated at a gating of 20 ns and 70% gain to resolve the formaldehyde excited by the laser.

Laser Mie Scatter imaging was utilized to visualize the RP-2 spray as the detonation wave traversed through it. A double pulse ND:YAG laser (532nm, 100 mJ) to illuminate the spray droplets. The laser sheet is generated at the center of the test section and the RP-2 spray. A Photron SA1 camera with 16-bit depth and a spatial resolution of 40 μm/pix was equipped with a 24-85mm F/3.5-4.5 Nikon Lens to capture the temporal evolution of the spray as it interacted with the detonation. A 532 nm bandpass optical filter attached to the lens with a Full-Width Half Maximum of 10 nm and transmission greater than 95% to capture the Mie scattering from 532 nm laser.

Four dynamic pressure transducers (PCB Model #113B26) are lined along the test section at intervals of 25mm to capture the pressure evolution. These transducers with a sensitivity of 10 mV/psi and uncertainty of 0.9-1.1% were operated at 1MHz to resolve the detonation and detonation-spray interaction pressures. A PCB 482C Series signal conditioner was used to amplify the signal for the NI DAQ and LabVIEW.

3. Results and Discussions

3.1 Detonation interaction with aerosolized liquid droplet RP-2 cloud.

The detonation evolution and interaction dynamics with the RP-2 spray cloud is shown in the sequence of images in Figure 5. The first two frames show the detonation wave incoming with a fully developed spray in front of it. Frame 1, where the detonation wave enters the test section, is at 0 μs. The first evidence of RP-2 burning is observed at 10 μs in Fig. 5(b) and 5(c), where the formation of CH* and CH_2O driven by RP-2 reaction regions are detected. The formation of the hydrocarbon reactions occurs as soon as the detonation wave interacts with the fringes of the spray, as portrayed in Fig. 5(a) at the 10 μs frame. The detection of CH* and CH_2O generation along the detonation front confirms RP-2 aerosolized droplet cloud burning since the detonation is supported by a hydrogen-air mixture and there should be no carbon species within the reaction front. However, because CH* and CH_2O are detected within the reaction front, the production of these species must come from the burning of the complex hydrocarbon molecules that make up RP-2. As the detonation wave propagates through the spray, the CH* and CH_2O reaction regions increase in width, signifying an increase in the size of the reaction front associated primarily with RP-2 droplet cloud burning. The largest structures for both CH* and CH_2O are seen at 40 μs. While it is observed that as the detonation propagates through the entirety of the test section from 0 to 40 μs and the CH* and CH_2O reaction regions increase in size proportionally to each time step, the intensity associated with both these reaches its maximum peak at 20 μs. From the schlieren images in Fig. 5(a) and the Mie scatter of the RP-2 aerosolized droplet cloud in Fig. 5(d), it is seen that the maximum peak intensity of these species occurs as the detonation wave has

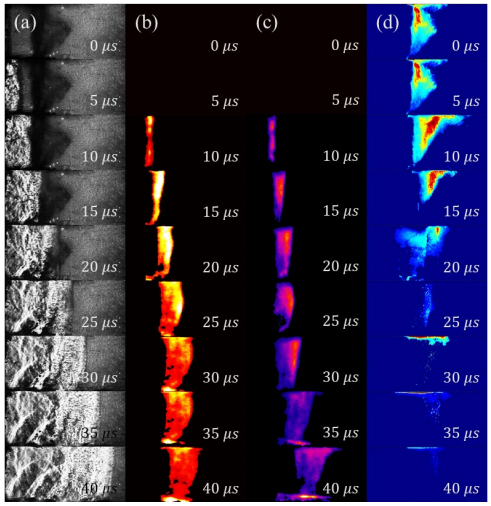

Fig. 5: Temporal evolution of the detonation wave propagation in a) schlieren b) CH* c) CH_2O PLIF d) Mie scatter

propagated approximately three quarters into the spray. Further validation of RP-2 burning as the detonation wave passes through the spray is provided by the Mie scatter imaging of the droplets, shown in Fig. 5(d). Observation of the droplet Mie scatter as the detonation wave propagates through the spray, less and less quantity of the spray exists. It is seen that by 40 μs, the spary is almost nonexistent. Thus, the Mie scatter, CH* chemiluminescence, and CH_2O PLIF provide clear evidence that the detonation wave is burning the RP-2 droplets within the wave front and evolving from a hydrogen-air to hydrocarbon reaction front.

3.2 Evidence of liquid driven detonation: Wave speed and pressure characterization

The propagation speed of the detonation wave was extracted from the schlieren images using the methods documented in [9, 10]. The spatial location of the shock front was defined and the displacement of the wave front is tracked over the frames relative to the 5 μs between each of the frames for the wave speed. The propagation velocity for the detonation wave is shown in Fig. 6(b); this figure displays the velocity evolution of the detonation wave and, in effect, captures its behavior as the wave interacts with the RP-2 spray.

As seen by the velocity profile, when the detonation wave first interacts with the fringes of the spray, minor RP-2 burn results in a slight wave speed increase between 5-10 μs. Immediately after, between 10-15 μs, it is seen that the wave speed drastically decreases as it propagates into the majority of the dense spray due to the momentum impartment, as portrayed in Fig. 6(b). The consumption of the dense spray leading to velocity deficit is seen in Fig. 6(a), where high-speed schlieren, PLIF, and Laser Mie Scatter have been superimposed. As the detonation propagates through the spray core a detonation velocity spike is experienced between 15-20 μs. This behavior is observed in Fig. 6(a), where the peak intensity of CH_2O species occurs, indicating maximum hydrocarbon burning. The wave then continues to burn through the remaining RP-2 spray nominally maintaining this higher propagation velocity until it starts to relax back down to the inlet wave speed. This behavior is consistent with the increase in peak pressure driven by the RP-2 burning as shown in Fig. 6(c). The pressure from the first two transducers before the injector show a nominally constant pressure of 300 psi which is the expected CJ pressure for the gaseous pre-filled mixture. However, the last two transducers show a significant pressure rise, approximately 200 psi increase. The source of this pressure increase stems from the combustion of RP-2 induced by the detonation wave.

A gaseous detonation with no spray interaction and a detonation with a water spray interaction case is also experimentally investigated for comparisons, as shown in Fig. 6(b) and 6(c). As expected, it is found that the gaseous test case is nominally constant for both wave speed and pressure at 1800 m/s and 300 psi, respectively. The case of the detonation interacting with the water spray also coincides with what is currently understood about detonations in that the wave speed is correlated to the heat release of the system. As such, a fluid such as water is expected to reduce the wave speed due to heat absorption and H_2O evaporation. This behavior is seen in Fig. 6(b), where the detonation wave interaction with the water spray decreases the wave speed from 1800 m/s to 1400 m/s. Inspection of the pressure trace from Fig. 6(c) also shows that as the detonation wave interacts with the water spray, the pressure decreases from 300 psi to approximately 150 psi as the detonation completely propagates through the spray. As the detonation wave leaves the spray and approaches the outlet of the test section, the pressure rises back to the nominal gaseous pressure seen at the inlet.

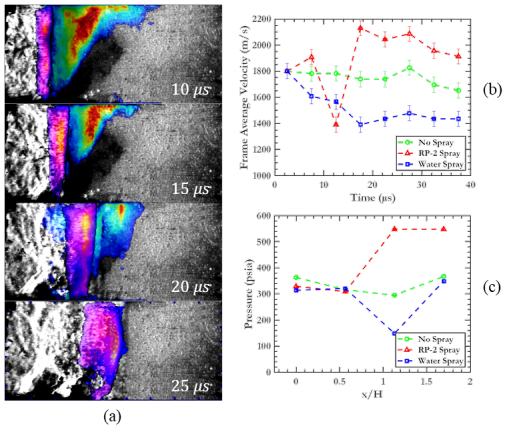

Fig. 6: Temporal evolution of the detonation wave speed. Pressure traces of test cases vary from gaseous, gaseous with RP-2 Spray, and gaseous with Water Spray. x/H = 0 refers to the first transducer.

3.3 Quantity of RP-2 combustion analysis

The Mie scatter images are further analyzed to quantify the diameters and counts of the droplets associated with the spray. The Mie scatter images are post-processed and edge detection applied to each individual droplet. These procedures are conducted in MATLAB, which utilized binarizing the images using Otsu's thresholding, high-pass filtering, contrast stretching, and morphological structuring algorithms to get a pixel diameter size associated with each droplet. Assuming perfectly spherical and axisymmetric droplets, the pixel volume was thus calculated. Total volume of the droplets is then calibrated using a catch and weight measurement of the injector, which allows the determination of the total volume from the mass and density of the liquid issued from the injector. Following this, the pixel diameter is of the droplets is then calibrated which

allows for an approximation of equivalent mass to be made for each frame. It is important to note that the goal of this procedure is not to characterize the injector but instead to document the effect driven by the detonation liquid burning using the Mie scatter images. Fig. 7 shows two chosen time frames for post-processing of the droplet sizes. The 10 μs represents the RP-2 spray before the detonation interaction, and the 25 μs is at the condition where the majority of the droplets have all been consumed. The resulting

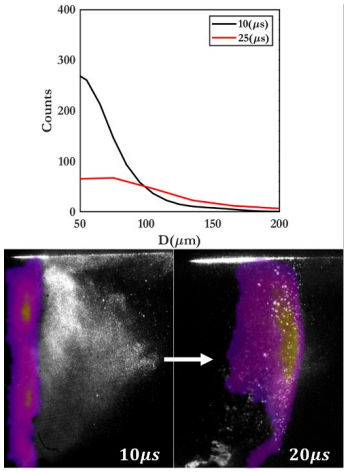

Fig. 7: Histogram of droplet distributions of the equivalent Mie scatter images.

histogram shows how the droplet distributions changed before and after spray interaction with the detonation wave. Initially, it is seen that the droplets have a much higher count than after, which coincides with the Mie scatter images. The majority of the smaller droplets are consumed and slight increase in the larger droplets is noticed due to coalescence. It is important to note that due to the resolution limitation, droplets smaller than 50 μm are not detected.

Using the distribution histograms, the total mass of the spray was calculated for each temporal frame relative to frame at 5 µs. The heat release associated with the chemical reactions is calculated via a method developed by Turns which allows approximation of the quantity relative to wave speed [12]. The frame-by-frame percent of mass recorded shows a near inverse trend compared to the velocity as portrayed in Fig. 8. Between 5-15 μs, the velocity decreases. Shortly after, the reaction increases sharply, which coincides with additional mass consumption and greater heat release. The exothermic driven reactions from the additional RP-2 leads to the explosive escalation of the velocity seen between 10-20 μs. As most of the leftover spray is consumed, the heat release and velocity experience a decay associated with the detonation wave relaxing down to its gaseous inlet velocity.

3.4 Induction zone analysis

Using Fig. 6a, which depicts the overlay of the schlieren and formaldehyde species, the spatial distance from the leading shock to the front, peak and trailing CH_2O PLIF signal is quantified. Fig. 9 depicts the length scales of the front, peak, and back locations

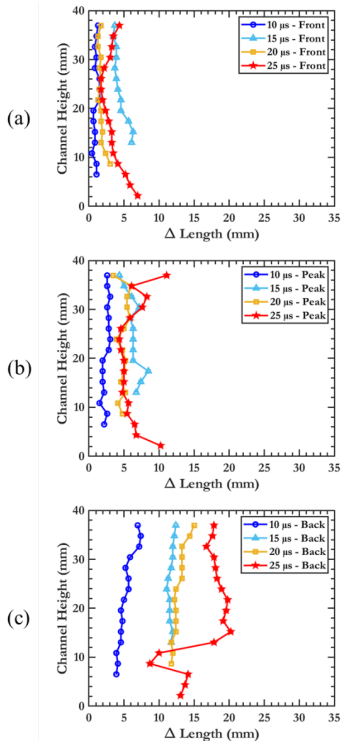

Fig. 9: Length scales associated with formaldehyde species formation relative to a) Front of a shock to the front of formaldehyde b) front of a shock to peak formaldehyde location conditions

for time frames of 10-25 μs. These computed distances indicate prominent delays for RP-2, such as the transient trend associated with where the burning starts, peak burning rate, and where the reactions terminate. In general, it is shown that initially, at 10 μs, the formaldehyde formation is coupled with the lead of the detonation indicating a short time delay for the reaction. However, as time progresses, a separation and then recoupling occurs. This potentially may be due to the sustenance of the detonation switching dominant fuel species combustion from hydrogen to hydrocarbon back to hydrogen. The documented results of Westbrook [13] agree with this trend since hydrocarbon detonations have considerably larger induction zone lengths than hydrogen detonations. This insight is counterintuitive as induction zone lengths are expected to decrease with increasing velocities due to higher post-shock temperatures. However, in this particular instance, that trend is not realized due to the influence of different fuel species on ignition delay and the inherent unsteady nature of a detonation propagating in a stratified liquid spray.

As the leading shock of the detonation wave interacts with the dense spray, the shock at specific locations disintegrates, mutating the shock complex to a large degree where they no longer have a conjoined planar structure across the entire channel. The tracking of the leading shock surface provides a marker of where the fragmentation of the structure is observed, particularly in frames 15 µs, 20 µs, and 25 µs, as shown in Fig. 9, which results in capturing the dominant structures for a fraction of the entirety of the channel height. Fig. 9b provides an assessment of the peak combustion intensities occurring near the front of the formaldehyde formation as the smaller droplets reacted in this length scale. On the other hand, the larger droplets take longer to reach complete combustion, which is why the distance from the front of the detonation to the back end of the formaldehyde formation continues to increase in length, as seen in Fig. 9c.

3.5 Idealized analysis of droplet detonation interaction

The experimental results show an increase in wave speed and pressure for the detonation interaction with the liquid RP-2 cloud. However, the short time scales of detonations prove sole implementation of the standard D^2 law to be insufficient as an explanation for observed experimental droplet size supporting the detonation [14, 15] therefore alluding to an alternative mechanism during the droplet-detonation interaction. Past findings report fine mist generation in the wake of the droplet [15-18] where Thomas [14] noted the mist or daughter droplets must be sub-micron due to their rapid evaporation rate. Nicholls, J. A., and A. A. Ranger [17] proposed a model to account for the generation of small droplets through boundary layer stripping in which a controlling parameter gives a ratio to the transit time and break up time scale. The stripped mass can be approximated by

$$\frac{m}{m_0} = (0.5)(1 + \cos \pi T/5)\ ,\ T = \frac{t_{det}\ u}{d}\sqrt{\frac{\rho_g}{\rho_l}}, \quad (1)$$

where m, m_0 are the mass final and initial droplet mass, and t_{det} is the time for the droplet to transit the detonation. A simplified schematic showing the impact of evaporating droplets on the detonation is shown in Figure 10. The detonation is treated as a leading shock followed by a reaction zone ending at the sonic plane. While further combustion may occur past the sonic plane it will not support the detonation. A simplifying assumption is that the only mechanism for mass transfer from the droplets is through boundary layer stripping and the stripped mass is evaporated before the reaction zone. It is also assumed that the velocity and temperature of the droplets is constant, the evaporated mass is decelerated and heated. The specific heat ratio is taken to be constant and induction length is unchanged from a detonation without liquid.

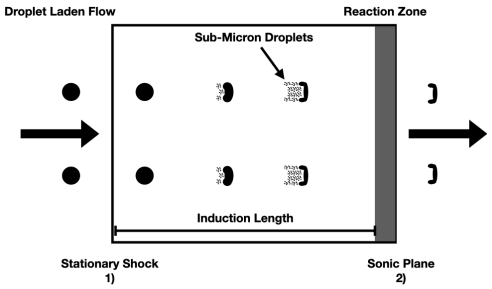

Figure 10: Schematic of the detonation shock followed by a reaction zone ending at the sonic plane. Droplets enter the detonation and begin to shed mass through boundary layer stripping that is burned in the reaction zone.

A key quantity of interest is how much of a droplet's mass is stripped and evaporated within the induction

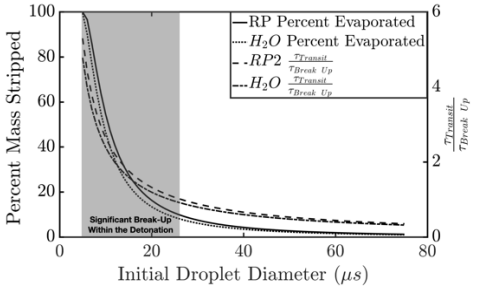

Figure 11: Percent mass stripped driven by the detonation for both RP-2 and Water.

length, as this is the only mass that will drive the detonation. Droplets will continue to break-up and evaporate after the sonic plane, likely burning in a deflagration reducing achievable detonation efficiency. The amount of mass stripped within a $H_2 - O_2 - N_2$ detonation at an equivalence ratio of 0.58 is presented in Figure 11. Wang et. al. [16] found for Mach 1.19 flow that break up is initiated at $T \sim 0.7$; suggesting that a significant portion of the distribution, marked in grey, will exhibit appreciable boundary layer stripping within the detonation.

The 0D model is applied to both the RP-2 and water cases to predict the change in detonation velocity with varying liquid volume fractions, Figure 12. The RP-2 case shows good agreement with the experimentally measured wave speed at the estimated volume fraction, whereas the water wave speed is over predicated. The lognormal distribution is based on experimental measurements for droplet diameters. While this is a very simple break-up model it has been previously shown to agree with experiments for

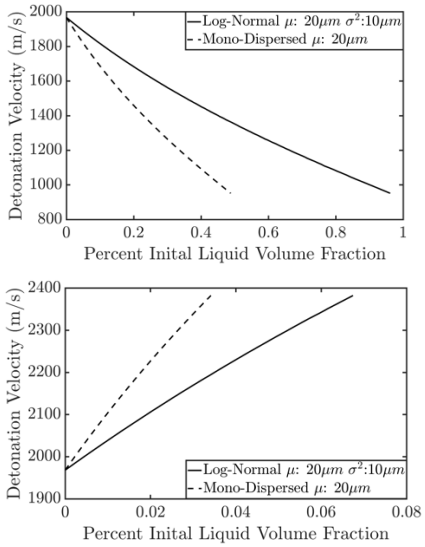

Figure 12: Model prediction of detonation velocity with lognormal and mono-dispersed distribution, μ:20 μm and σ^2:10 μm, droplets at varying initial liquid volume fractions. Detonation velocity for two different liquids, (Top) water and (Bottom) RP-2

droplets ranging from 290-2600 microns [11]. The 0-D model along with previous work provides some evidence that boundary layer stripping of micron to sub-micron droplets is a candidate mechanism for conversion of liquid to vapor within detonation time scales. Further analysis is needed to account for any changes in the detonation thickness as well as variation in droplet velocity.

4. Conclusion

This research characterized the RP-2 spray interaction with an incoming gaseous detonation. Evidence of RP-2 burning is provided via High-speed experimental Schlieren, Ch*Chemiluminescence, Formaldehyde Planar Laser-Induced Fluorescence (PLIF), and Laser Mie Scatter. Dynamic pressure measurement and wave speed calculation show an increase in both pressure and wave speed when the detonation wave interacts with RP-2 spray. This increase in pressure and wave speed confirms that a liquid fuel spray supports an incoming detonation. Utilization of the Nicholls, J. A., and A. A. Ranger detonation droplet interaction breakup model allows accounting for boundary layer stripping which shows good agreement between experimental and theorical wave speed attained for water and RP-2. This provides preliminary evidence that boundary layer stripping may cause the formation of micron to sub-micron droplets as a viable candidate mechanism for conversion of liquid to vapor in required detonation time scales.

Acknowledgements

The work is sponsored by the Air Force Office of Scientific Research support under award 19RT0258/FA9550-19-0322 by Program Manager Dr. Chiping Li. Dr. Li was behind the idea of the investigation, and provided insightful inputs and suggestions for computing the liquid droplet burnout time, liquid mass consumption, and heat release.

References

[1] K. Kailasanath, Review of Propulsion Applications of Detonation Waves, *AIAA Journal*, 38 (2000) 1698-1708.

[2] J.A.D. Nicholls, E. K, Recent results on standing detonation waves, *Symp. Combust*, 8 (1961) 644-655.

[3] F.A. Williams, Structure of Detonations in Dilute Sprays, *Physics of Fluids*, 4 (1961).

[4] K.W. Ragland, Observed Structure of Spray Detonations, *Physics of Fluids*, 11 (1968).

[5] G. Yao, B. Zhang, G. Xiu, C. Bai, P. Liu, The critical energy of direct initiation and detonation cell size in liquid hydrocarbon fuel/air mixtures, *Fuel*, 113 (2013) 331-339.

[6] M.A. Benmahammed, B. Veyssiere, B.A. Khasainov, M. Mar, Effect of gaseous oxidizer composition on the detonability of isooctane–air sprays, *Combustion and Flame*, 165 (2016) 198-207.

[7] G. Jarsalé, F. Virot, A. Chinnayya, Ethylene–air detonation in water spray, *Shock Waves*, 26 (2016) 561-572.

[8] H. Watanabe, A. Matsuo, A. Chinnayya, K. Matsuoka, A. Kawasaki, J. Kasahara, Numerical analysis of the mean structure of gaseous detonation with dilute water spray, *Journal of Fluid Mechanics*, 887 (2020).

[9] H.M. Chin, J. Chambers, J. Sosa, A. Poludnenko, V.N. Gamezo, K.A. Ahmed, The evolution of pressure gain in turbulent fast flames, *Combustion and Flame*, 234 (2021).

[10] A.Y. Poludnenko, J. Chambers, K. Ahmed, V.N. Gamezo, B.D. Taylor, A unified mechanism for unconfined deflagration-to-detonation transition in terrestrial chemical systems and type Ia supernovae, *Science*, 366 (2019).

[11] S.A. Gubin, M. Sichel, Calculation of the Detonation Velocity of a Mixture of Liquid Fuel Droplets and a Gaseous Oxidizer, *Combustion Science and Technology*, 17 (2007) 109-117.
[12] S.R. Turns, An Introduction to Combustion Concepts and Applications, McGraw-Hill, 2012.
[13] C.K.U. Westbrook, P. A, Chemical-Kinetic Prediction of Critical Parameters in Gaseous Detonations, *Int. Symp. Combust*, (1982).
[14] G.O. Thomas, M.J. Edwards, D.H. Edwards, Studies of Detonation Quenching by Water Sprays, *Combustion Science and Technology*, 71 (1990) 233-245.
[15] E.K. Dabora, K. W. Ragland, and J. A. Nicholls, Drop-size effects in spray detonations, *Symposium (International) on Combustion*, Vol. 12. No. 1 (1969).
[16] Z. Wang, T. Hopfes, M. Giglmaier, N.A. Adams, Effect of Mach number on droplet aerobreakup in shear stripping regime, *Exp Fluids*, 61 (2020) 193.
[17] J.A. Nicholls, A.A. Ranger, Aerodynamic shattering of liquid drops, *AIAA Journal*, 7 (1969) 285-290.
[18] D.D. Joseph, J. Belanger, and G. S. Beavers, Breakup of a liquid drop suddenly exposed to a high-speed airstream, *International Journal of Multiphase Flow*, 25.6-7 (1999) 1263-1303.